ngVLA Antenna Memo # 6

Efficiency Loss due to Feed Positioning Errors on the ngVLA Reference Design Antenna

Sivasankaran Srikanth, Central Development Laboratory, Charlottesville, VA

April 7, 2020.

Abstract

This memo presents effects of feed positioning errors on the ngVLA shaped antenna (Version 6). The efficiency loss and increase in crosspolarization are shown. The analysis was carried out in the 12.5 to 21.5 GHz band, covering most of the Band 3 frequency range (12.3 to 20.5 GHz). Simulated patterns of an axially corrugated feed horn were used in the GRASP software to compute the antenna patterns and efficiency. Results presented here agree closely with simulations performed at 15.0 GHz by EMSS Antennas. All results shown here are directly scalable to other ngVLA bands. Efficiency for dual-offset Gregorian antennas with three different subreflector angles is also shown. An exploration of a design with improved off-axis performance is suggested for the ngVLA antenna. Feed position error is often referred to as feed offsets in this memo.

1 Introduction

Radio telescopes operating in the centimeter wavelengths typically have subreflector opening angles θ_s (half angle) varying between 10º and 20º. These telescopes have main reflectors that are at least 25 m in diameter and may be as large as 100 m. The most efficient feeds for such telescopes are the linear taper corrugated horns with narrow flare angles $\theta_f \leq 20º$. These horns have aperture diameters $\geq 8\lambda$ (at the low frequency end) and have over 2:1 bandwidth. Secondary focus receivers at lower bands use profile/compact horns. These horns are about 35% smaller in aperture diameter and 25% shorter in length, compared to a linear taper horn for a given illumination taper. The aperture diameters are usually $\geq 4.5\lambda$. In the case of aperture synthesis telescopes, the antenna diameters are often ≤20 m, for facilitating close packing of the elements. The antenna diameters, in the case of the MeerKAT [1] and the DVA-1 [2], one of the prototypes for the Square Kilometer Array (SKA) project are 13.5 m and 15 m, respectively. In these two projects, the antenna optics chosen uses wide angle subreflectors with $\theta_s \geq 45º$ in order to keep the feed size small. Wide flare angle axially corrugated horns (ACH) [3], [4] and/or quad-ridged flared horns [5] are the choice of feeds for these telescopes. These horns have aperture diameters $\leq 4\lambda$.

2 ngVLA antenna optics

The chosen diameter for the ngVLA antenna is 18 m, mostly for reasons of (a) cost to meet point source sensitivity and (b) survey speed. The ngVLA, as well as the other projects, use dual-offset Gregorian optics for reasons of higher gain, lower sidelobe levels, minimized standing waves and blockage-free large real estate that can house all the receivers. The subreflector is 3.5 m in diameter (14λ at the lowest frequency of operation) and has $\theta_s = 55º$. When the main reflector offset distance is about half its diameter in the case of dual-offset Cassegrain antenna, the subreflector introduces blockage of the aperture. The blockage is bigger for wider subreflector angles. Hence, the choice of Gregorian optics.

The reference design for the ngVLA antenna uses shaped optics that provides high illumination efficiency and low spillover but allowing higher than typical near-in sidelobes. A high efficiency mapping function was developed [6] and Figure 1(a) shows the cross section in the symmetry plane and the rays in the aperture plane that emanate from the focus. A dual-offset Gregorian antenna that was the basis for the shaped system is shown in Figure 1(b).

3 Efficiency loss as a result of feed position error

The six receivers called for in the proposal [7] are housed in two cryostats. Receiver selection is done by linear translation of the cryostat housing, which has freedom of movement in three directions. Figure 2 shows the translation coordinate system where, the X_fZ_f plane is the symmetric plane of the antenna. Z_f is along the feed axis pointing towards the subreflector and X_f is towards the center of the main reflector aperture. Analysis of the effect of error in feed positioning with respect to the secondary focus on efficiency was carried out at frequencies between 12.5 and 21.5 GHz. The feed is offset by 2.5, 5 and 7.5 cm in both the symmetric plane ($\pm X_f$ and $\pm Z_f$ directions) and perpendicular to the symmetric plane, which is referred to as the asymmetric plane in this memo (Y_f direction). These position errors are 1λ, 2λ and 3λ at 12.5 GHz.

An axially corrugated wide flare horn designed by L. Baker [4], was scaled to Band 3 and used in the present analysis. Simulated feed patterns at 12.5 GHz and 21.5 GHz are shown in Figure 3. The feed patterns show excellent circular symmetry up to19.5 GHz, with crosspolarization maximum at -30 dB. There is loss of symmetry at higher frequencies and crosspolarization is -27 dB at 21.5 GHz. A spherical wave expansion representation of the fields of the above feed horn was used in GRASP to calculate the antenna beam patterns. Calculated beam patterns of the antenna at 15.5 GHz are shown in Figure 4, for feed at focus (a) and for the three different offsets in (b), (c) and (d) in Y_f direction. For the on-axis case, patterns are shown in three different planes. In the offset cases, copol pattern is shown in the plane of the offset and the direction of the beam peak and gain values are indicated. For larger offsets, the gain is lower, and the main beam distorts by a larger amount. The purple curve is the crosspolarization caused by the feed polarization in the 45º-plane. The cyan curve is antenna induced crosspolarization and it deteriorates from -45 dB when the feed is at focus to -32 dB for a 7.5 cm offset. Figure 5 shows beam patterns for offsets in the X_f direction and are very similar to patterns in Figure 4. The feed offsets in this direction does not affect the antenna induced crosspolarization. Antenna beam patterns for feed offsets along the feed axis (towards the subreflector) are shown in Figure 6. The nulls between the sidelobes are filled in and even for 2.5 cm offset, the gain has dropped by more than 3 dB, substantial drop compared to the other two cases. Beam patterns for offsets in the $-X_f$ and $-Z_f$ directions where beam distortion is less severe, are not shown for brevity.

Aperture efficiency as a function of frequency for different offsets are shown in Figures 7, 8 and 9. The red trace is the efficiency for the feed at the focus and varies between 0.86 and 0.89. Efficiency for a given feed offset is nearly the same in the positive and negative X_f directions as seen in Figure 8 at almost all frequencies. Again, efficiency for offsets in Y_f direction (Figure 7) is almost identical as that for offsets in X_f direction. This is also clear from the efficiency plot in Figure 10, where the variation is shown at 15.5 GHz and 20.5 GHz, Figures 10 (a) and 10 (b), respectively. The change in efficiency as a function of frequency is higher for offsets in the $+Z_f$ direction, compared to $-Z_f$ direction as shown in Figure 9. Again, the loss in efficiency for offsets is much higher along the Z_f axis, compared to the other two directions. Figure 11 shows normalized efficiency for offsets in the three directions. For an offset of 2.5 cm, the loss at 15.5 GHz is about 7% along X_f and Y_f directions and 52% along Z_f and at 20.5 GHz, the loss is 11% (X_f, Y_f) and 64% (Z_f). For feed positioning error of 1λ in the Z_f direction, the loss in efficiency is greater than 50%, which is equivalent to observing with only half the number of elements in

the array. For Band 6 receiver, the positioning mechanism in the Z_f direction should be $\leq \pm 2$ mm, in order to keep the efficiency loss $\leq 25\%$. This large loss in efficiency can be mitigated by resorting to smaller angle subreflectors, as shown in the following section. Contract work on tolerance analysis was carried out by EMSS Antennas [8]. Figure 12 shows their results at 15 GHz and is in excellent agreement with NRAO results, excepting that the plot in the Z direction is reversed.

4 Efficiency loss in dual-offset Gregorian antennas with θ_s=55º, 46º and 41º

Figure 13 shows three designs of Gregorian antennas with θ_s=55º, 46º and 41º [9]. The sizes of the subreflectors are about the same for the three cases, 3.2 m x 3.4 m. The smaller the θ_s, the longer the focal length of the ellipsoid and larger the feed to subreflector distance. Band 3 feed horns that provide an illumination taper of about -13 dB at the subreflector edge of the three Gregorian antennas are shown in Figure 14. The flare angles θ_f for the horns are 55º, 45º and 40º for the θ_s=55º, θ_s=46º and θ_s=41º antennas, respectively. The 40º feed horn is about 1.5 cm larger in aperture compared to the 55º feed horn. Feed patterns at 12.5 GHz and 21.5 GHz are shown in Figures 15 and 16, for the two horns with θ_f=45º and 40º, respectively. The patterns of the 40º horn show excellent circular symmetry of the beam all the way to 21.5 GHz, while the other two horns lose their symmetry around 19.5 GHz.

The offsets used here are similar to that used in Section 3, with Z_f along the feed axis. Antenna beam patterns at 15.5 GHz for feed offsets of 7.5 cm in the three directions are shown in Figures 17, 18 and 19, for the three antennas. The beams for the feed at focus cases are also shown. Gain values are shown for each case and loss in gain is smaller and the deformation of the beam is less severe, for the lower θ_s antenna. The coma lobe levels are -13 dB, -17 dB and -20 dB below the peak for the three antennas. The antenna induced crosspolarization (cyan curves in (b)) is -31 dB, -33 dB and -34 dB, for the θ_s=55º, θ_s=46º and θ_s=41º antennas, respectively. Normalized efficiency for the ngVLA antenna is compared with that of the three Gregorian antennas in Figures 20, 21 and 22, in Y_f, X_f and Z_f directions respectively. The results for offsets in the Y_f direction presented here are also shown in Figure 28 of the ngVLA Antenna Memo # 4 [9]. The average efficiency for offsets of 2.5 cm and 5.0 cm are given for each case. The ngVLA antenna has offset losses two times and one-half times larger than the θ_s=55º Gregorian antenna in the Y_f and X_f directions. However, in the Z_f direction the loss due to feed offset is higher for the Gregorian antenna. Most of the loss is due to increased spillover. The losses decrease with decreases in θ_s and for the θ_s=41º antenna, the loss is <5% for offsets up to 5.0 cm in the Y_f and X_f directions. Also, the loss is at least three times lower compared to the θ_s=55º antenna. In the Z_f direction, the θ_s=41º antenna has much lower loss compared to the ngVLA antenna and two times lower loss compared to the θ_s=55º antenna.

Figures 23, 24 and 25 are for the same data as in Figures 20, 21 and 22, respectively, except the plots show absolute efficiency values. The θ_s=41º Gregorian antenna has substantially lower loss for offsets all the way to 7.5 cm in the X_f and Y_f directions, compared to the other cases. For offsets $\geq$5 cm, this antenna has even higher efficiency compared to the ngVLA shaped antenna for frequencies $\geq$15.5 GHz. In the Z_f direction, for an offset of 2.5 cm, the θ_s=41º Gregorian antenna has 5 to 10% higher efficiency compared to the ngVLA antenna.

5 Conclusions

Efficiency loss due to feed positioning errors of 2.5 cm, 5 cm and 7.5 cm, has been computed at most of the ngVLA Band 3 frequencies. In the plane orthogonal to the feed axis, for an offset of 2.5 cm, the loss is 7% at 15.5 GHz. However, along the feed axis the loss for the same offset is 52%. The ngVLA antenna is very sensitive for feed offsets along feed axis. Results of this analysis when scaled to Band 6, requires the feed to be positioned better than ±2 mm along the feed axis for efficiency loss $\leq$25%. The

ngVLA antenna exhibits poorer performance for offsets in the plane perpendicular to the feed axis compared to a Gregorian antenna with same θ_s; however, has better performance for offsets along the feed axis. Analysis of efficiency for Gregorian antennas with θ_s=55º, 46º and 41º shows, that loss in efficiency reduces by three times between the 55º and 41º antennas for offsets in the plane perpendicular to the feed axis, and by two times along the feed axis. As similar results are expected for shaped antennas, the stringent feed positioning requirements on the current design of the ngVLA antenna could be relaxed by exploring designs with $\theta_s \leq 41^o$. In case of the reference design, if the feed offset along the feed axis is more than 1λ, the resulting loss in efficiency is equivalent to a loss of between 100 – 120 antennas in the 244-element array.

The author acknowledges the comments and edits suggested by P. Ward, R. Selina and E. Murphy.

References

[1] I. P. Theron, R. Lehmensiek and D. I. L. de Villiers, "The design of MeerKat dish optics," 2012 International Conference on Electromagnetics in Advanced Applications, September 2-7, 2012.
[2] G. Cortes, W. Imbriale and L. Baker, "DVA-1 Optics Design and Analysis," DVA1_CDR_Optics_V3_2012_06_17.
[3] R. Lehmensiek and D. I. L. de Villiers, "Wide Falre Angle Axially Corrugated Conical Horn Design for a Classical Offset Dual-Reflector Antenna," 6th European Conference on Antennas and Propagation (EUCAP) 2012.
[4] L. Baker and B. Veidt, "DVA-1 Performance with An Octave Horn from CST and GRASP Simulations," octave_horn_rpt.nb, 03/30/2014.
[5] J. Shi, S. Weinreb, W. Zhong and X. Yin, "Quadruple-Ridged Flared Horn Operating from 8 to 50 GHz," Internal Memo, Dept. of Electrical Engineering, California Institute of Technology, Pasadena, CA, December 1, 2016.
[6] L. Baker, "Analysis of ngVLA Design #6 With Ideal and Actual Feed," Document #: 020.25.01.00.00-0001-REP ngVLA Optical Reference Design, January 2017.
[7] W. Grammer et al., "ngVLA Front End Reference Design Description," Document # 020.30.03.01.00-0003-DSN.
[8] R. Lehmensiek and D. I. L. de Villiers, "Tolerance Study (Order #: 364523)," October 2019.
[9] S. Srikanth, "Performance of Dual-Offset Gregorian Antennas with varying Subreflector Angles," ngVLA Antenna Memo # 4, July 18, 2019.

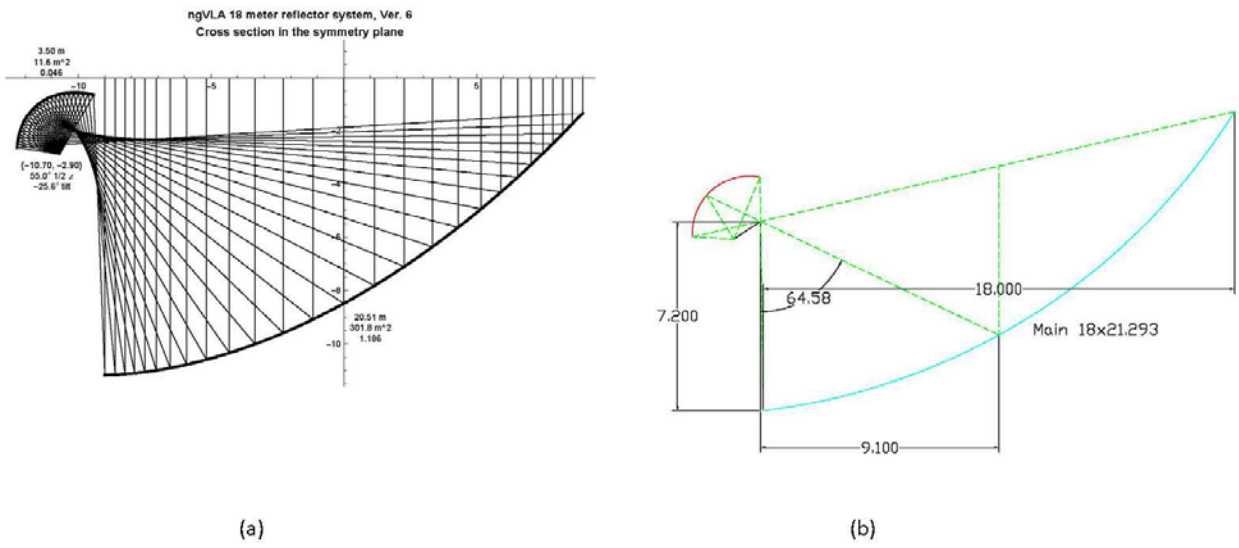

Figure 1. (a) ngVLA shaped antenna, (b) Equivalent Gregorian antenna.

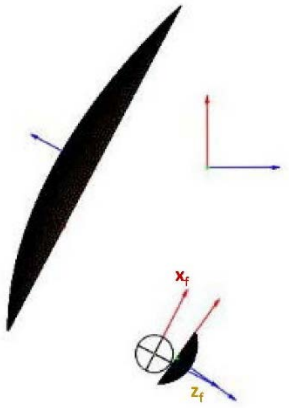

Figure 2. Coordinates of the ngVLA feed system.

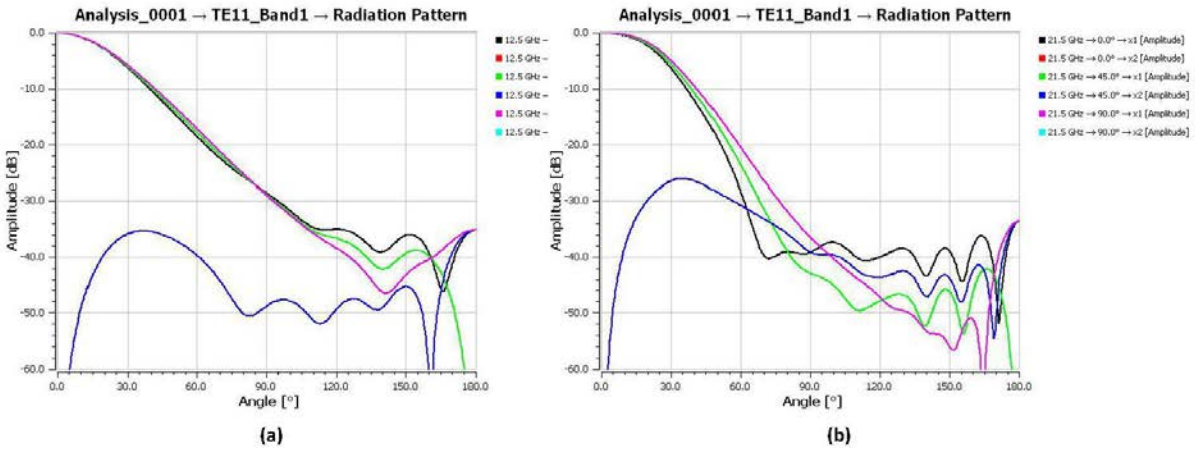

Figure 3. Axially corrugated feed horn patterns in three planes (a) 12.5 GHz, (b) 21.5 GHz.

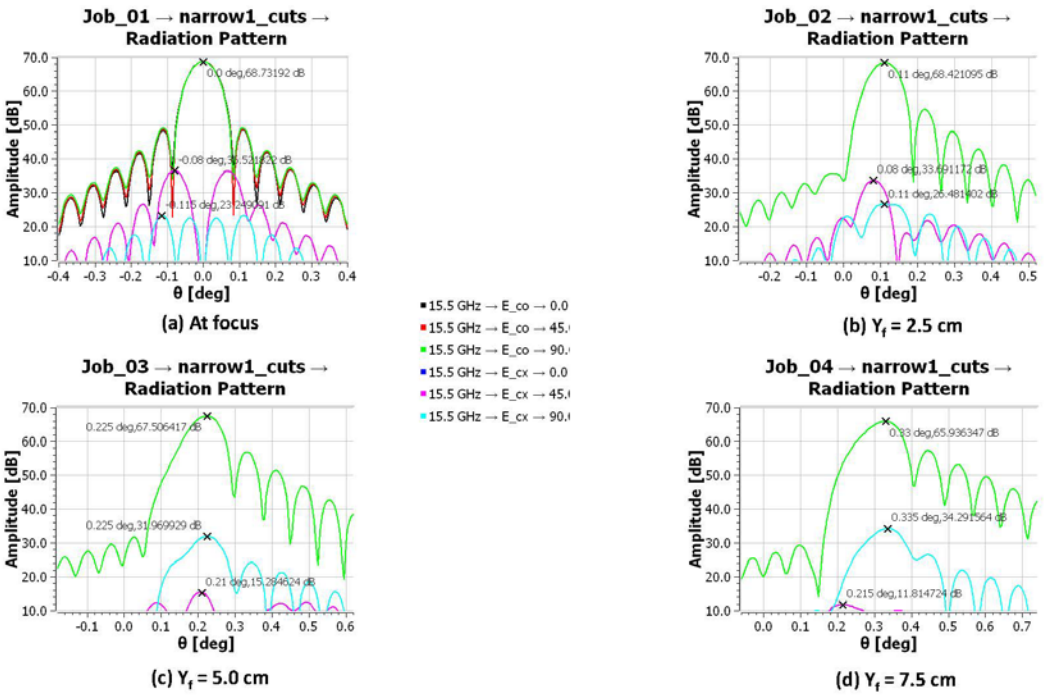

Figure 4. Antenna beams for feed position errors in the asymmetric plane (Y_f direction).

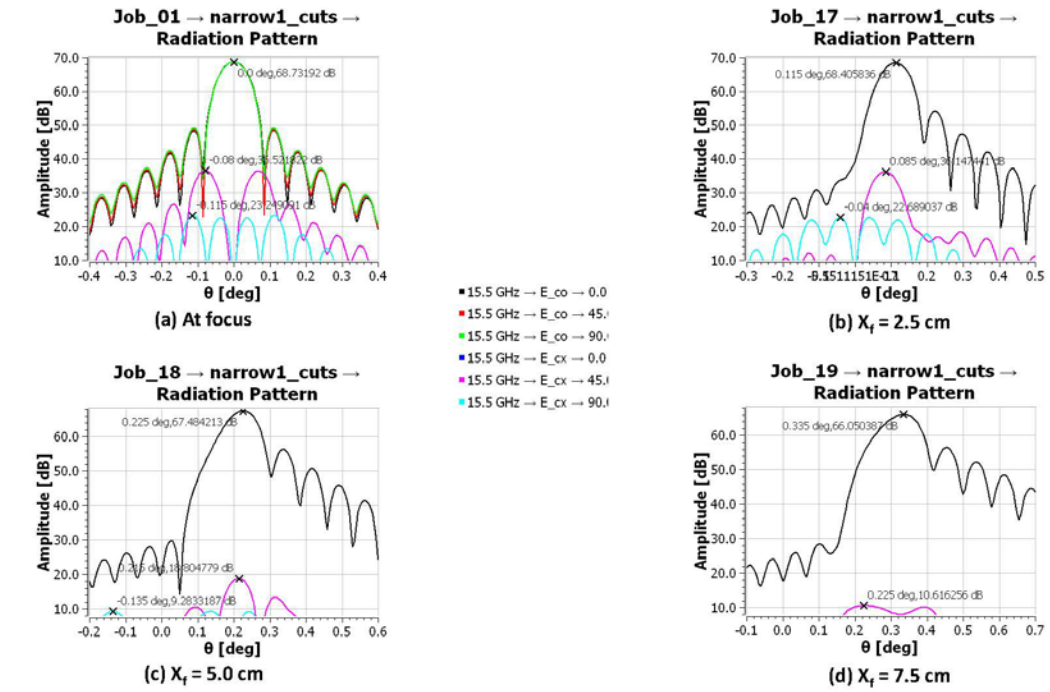

Figure 5. Antenna beams for feed position errors in the symmetric plane (X_f direction; towards aperture center).

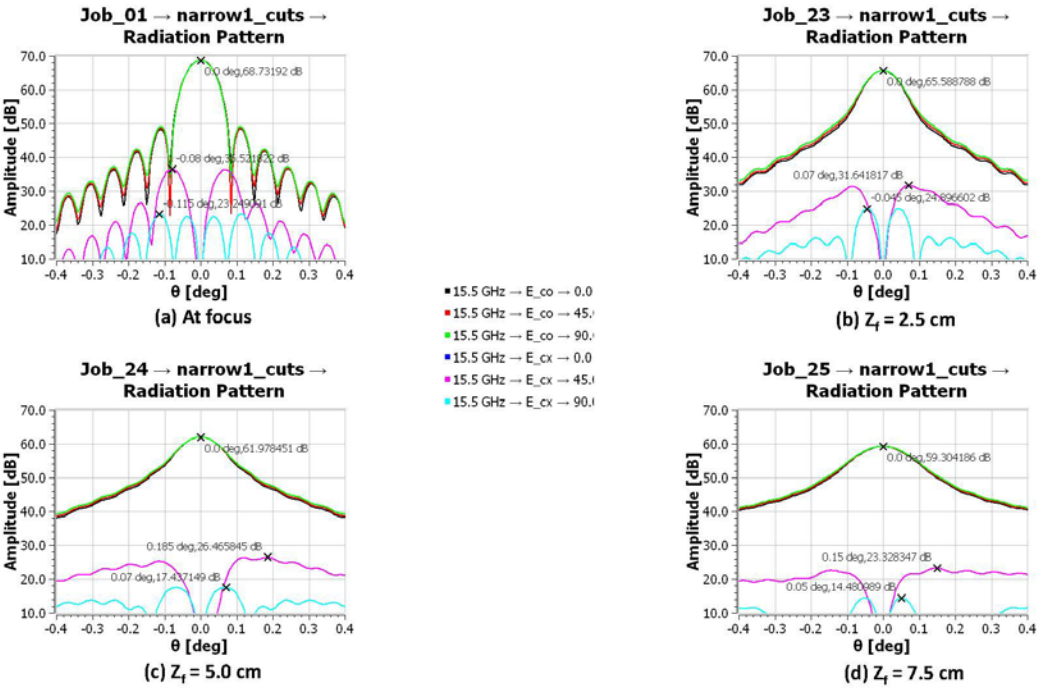

Figure 6. Antenna beams for feed position errors along feed axis (Z_f direction; towards subreflector).

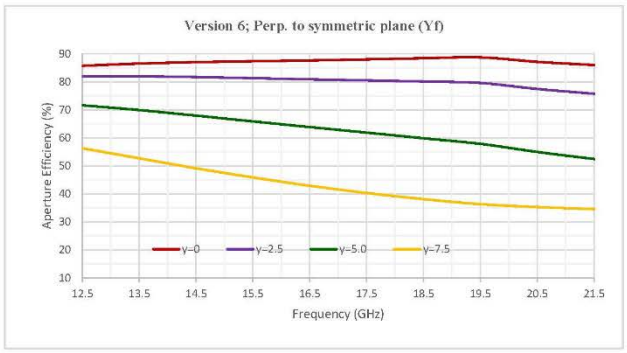

Figure 7. Aperture efficiency for offsets in the asymmetric plane (Y_f direction).

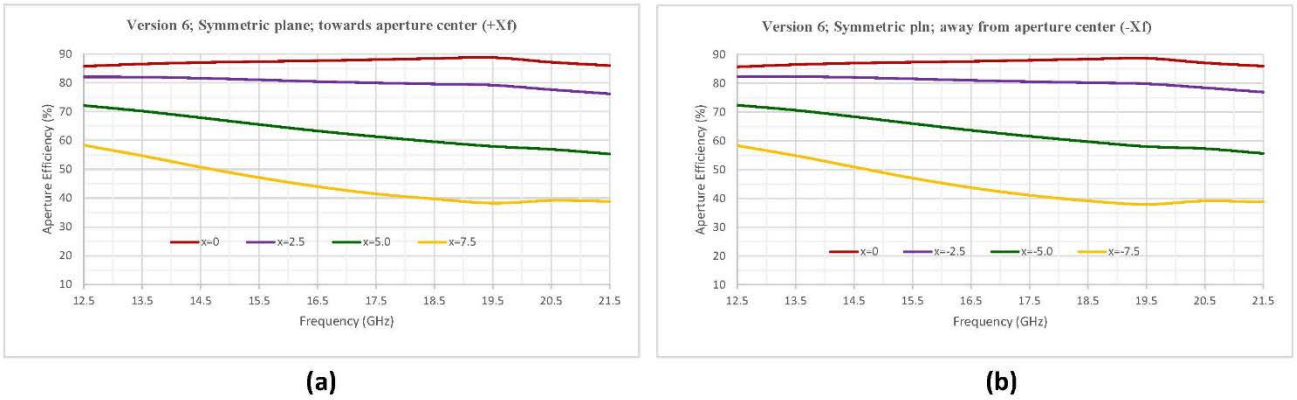

Figure 8. Aperture efficiency for offsets in the symmetric plane (a) $+X_f$ direction, (b) $-X_f$ direction.

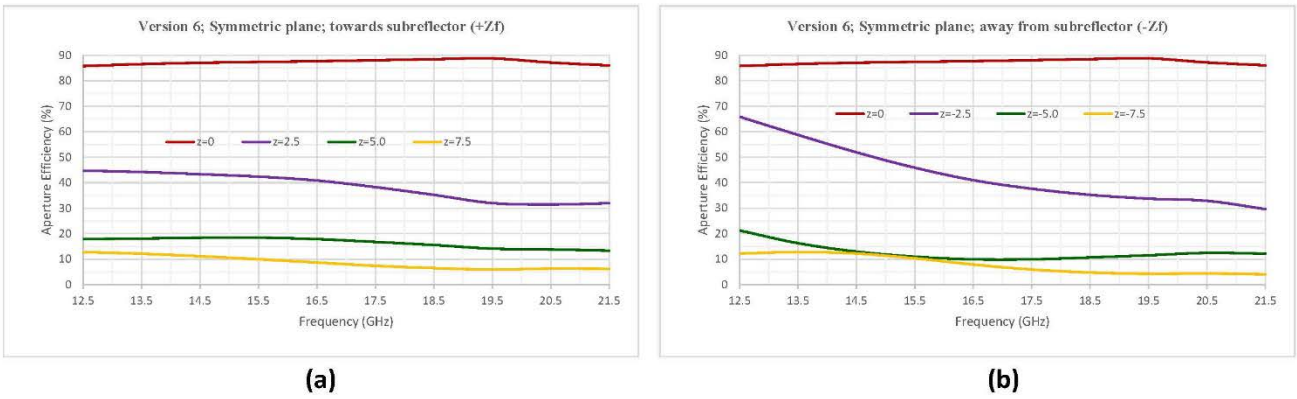

Figure 9. Aperture efficiency for offsets in the symmetric plane (a) $+Z_f$ direction, (b) $-Z_f$ direction.

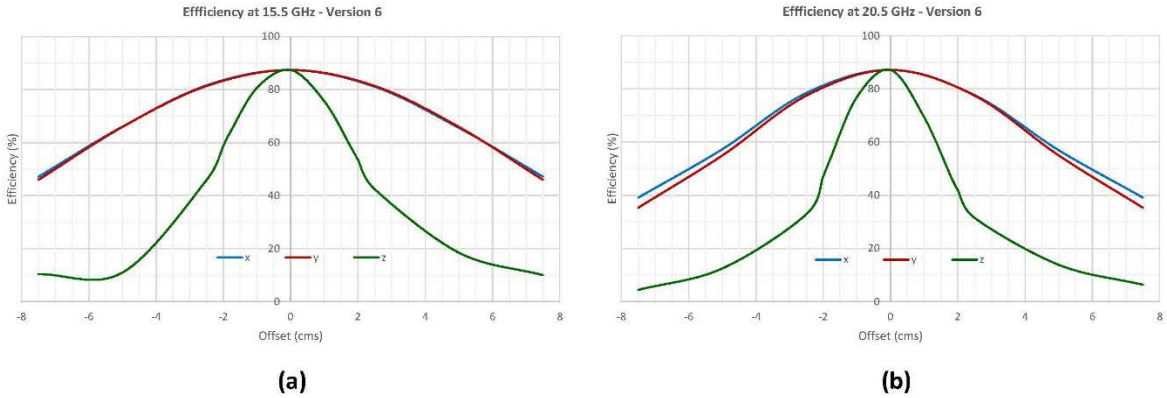

Figure 10. Aperture efficiency for offsets in $\pm X_f$, $\pm Y_f$ and $\pm Z_f$ directions (a) 15.5 GHz, (b) 20.5 GHz.

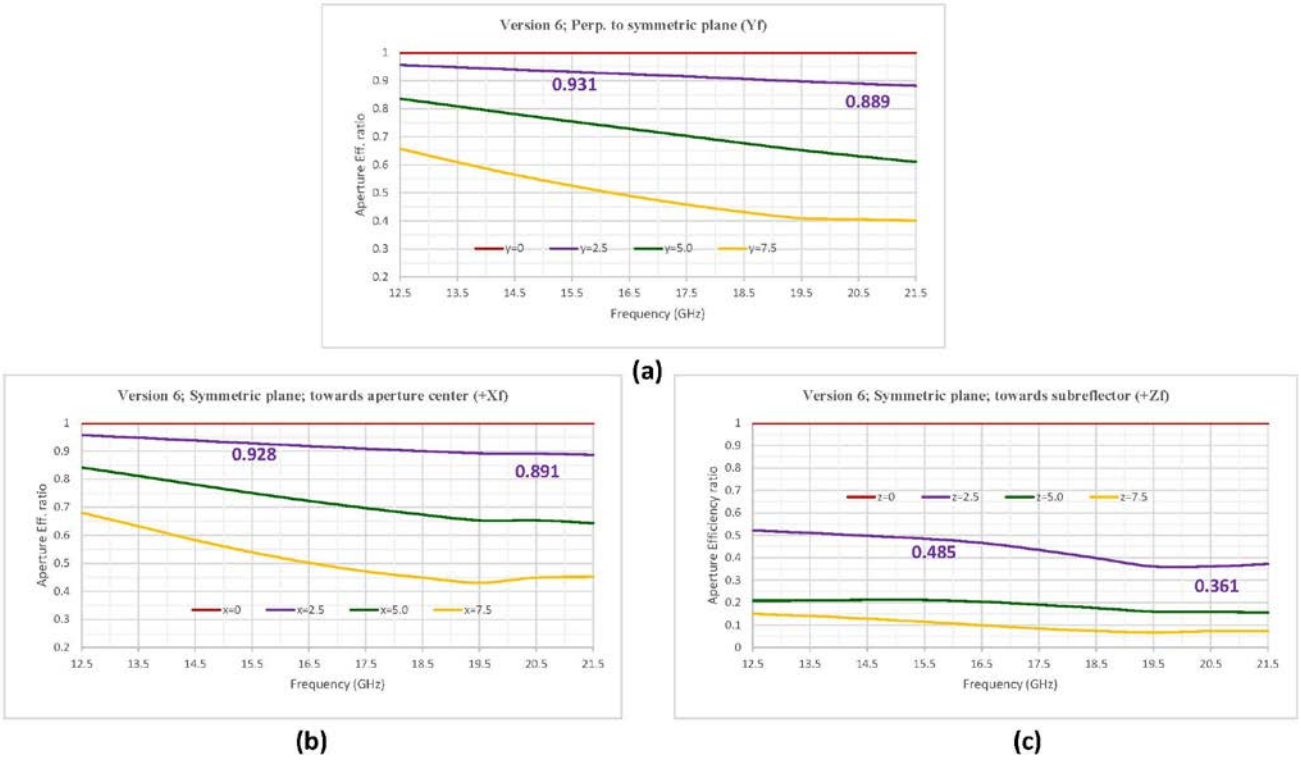

Figure 11. Normalized aperture efficiency for offsets along (a) $+Y_f$, (b) $+X_f$, (c) $+Z_f$.

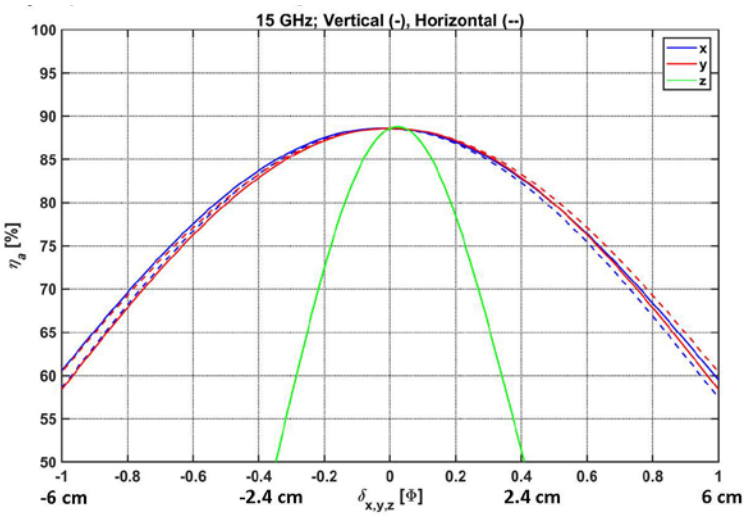

Figure 12. Aperture efficiency for offsets in $\pm X_f$, $\pm Y_f$ and $\pm Z_f$ directions at 15.0 GHz (EMSS Antennas).

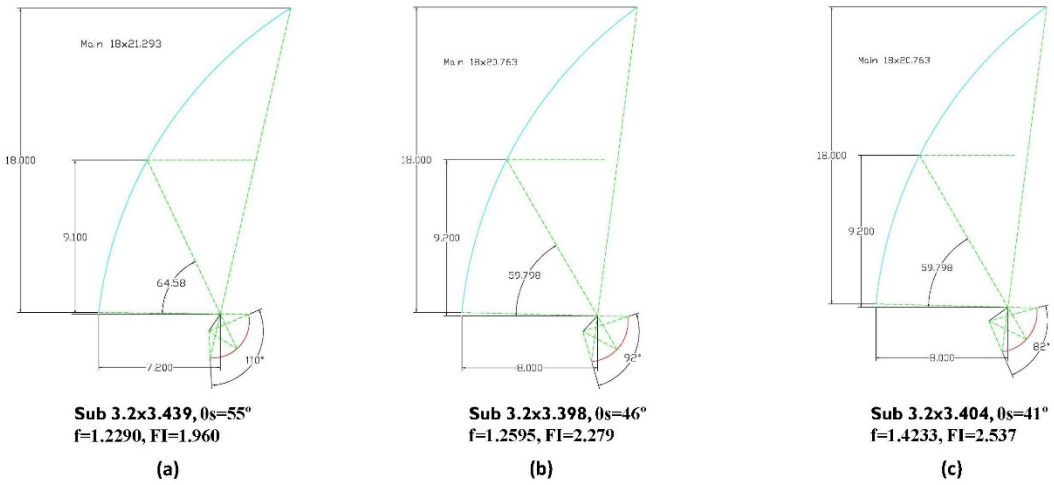

Figure 13. Dual-offset Gregorian antennas with (a) θ_s=55º, (b) θ_s=46º, (c) θ_s=41º.

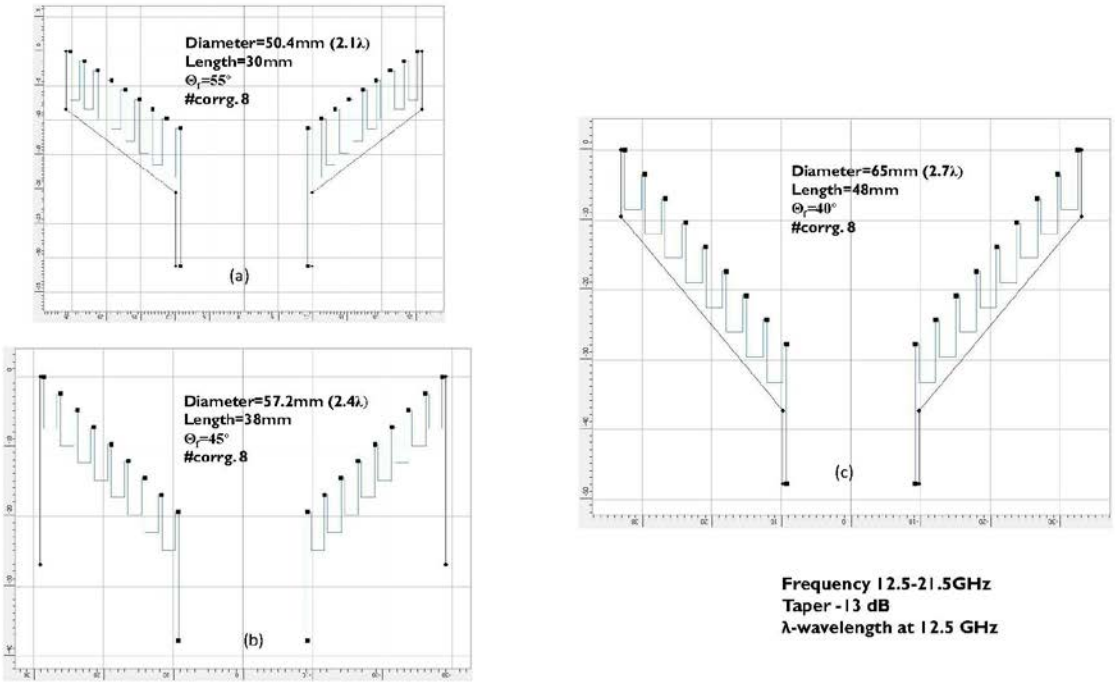

Figure 14. Axially corrugated feed horns (12.5 – 21.5 GHz) for (a) θ_s=55º, (b) θ_s=46º, (c) θ_s=41º.

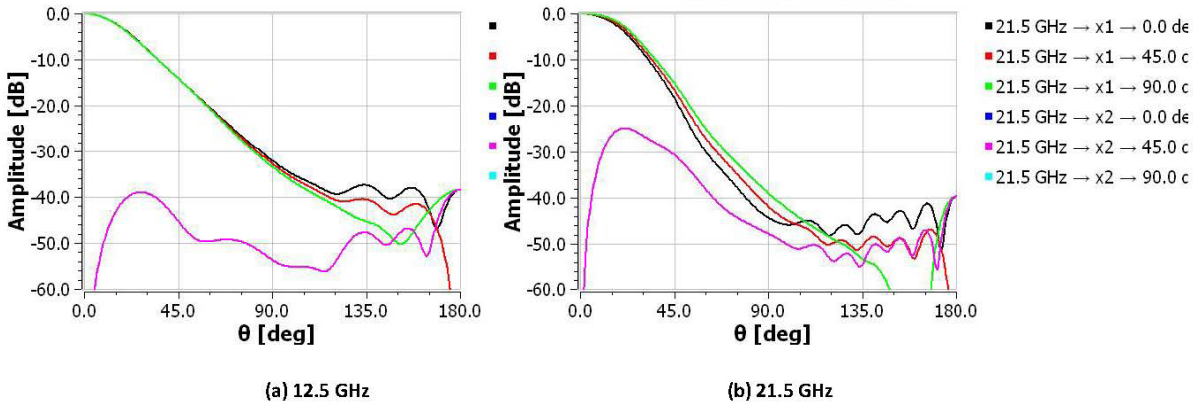

Figure 15. Axially corrugated feed horn (θ_f=45º) patterns (a) 12.5 GHz, (b) 21.5 GHz.

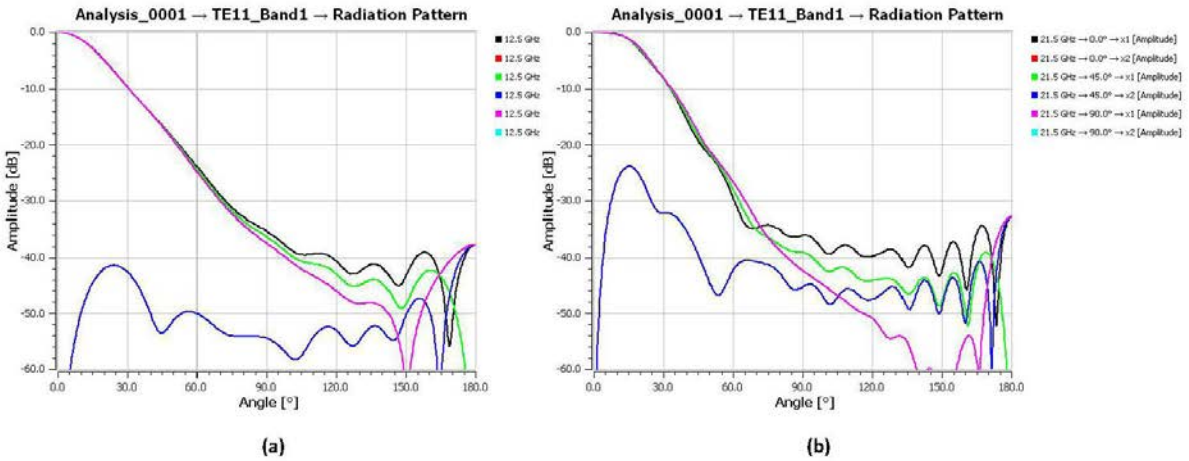

Figure 16. Axially corrugated feed horn (θ_f=40º) patterns (a) 12.5 GHz, (b) 21.5 GHz.

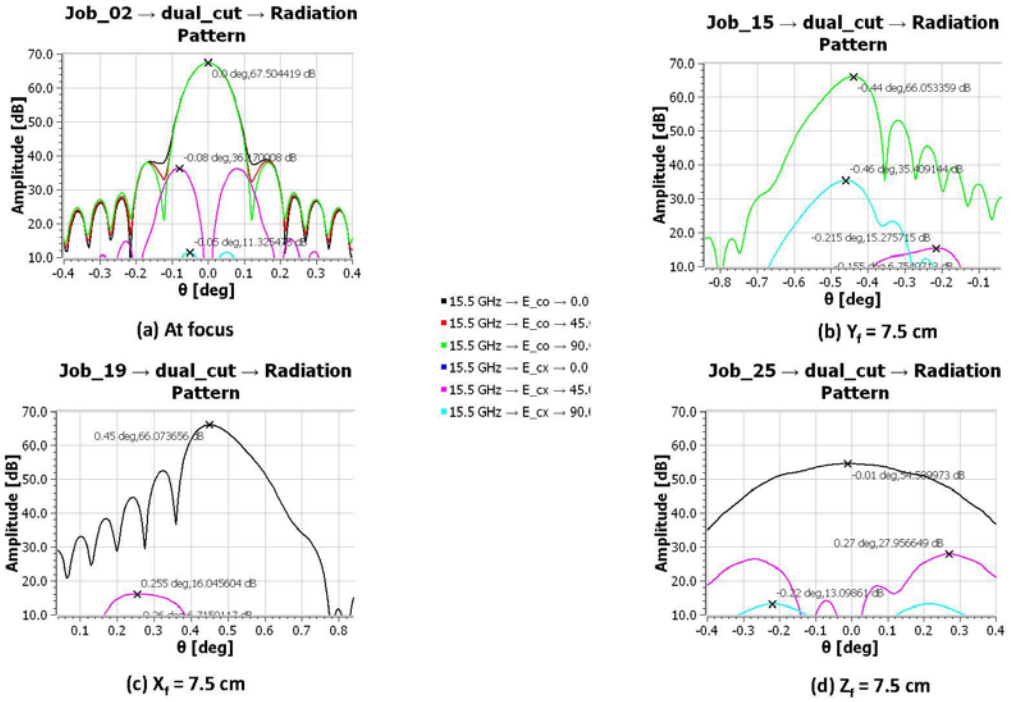

Figure 17. Beams of Gregorian antenna with θ_s=55º for feed position error of 7.5 cm (a) at focus, (b) Y_f, (c) X_f, (d) Z_f direction.

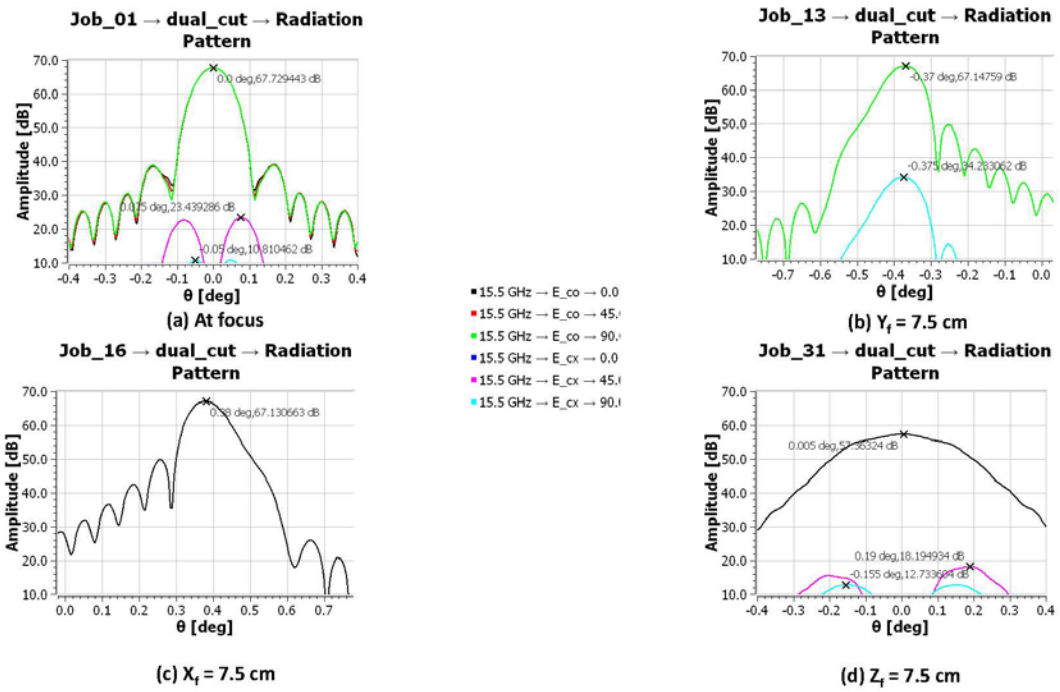

Figure 18. Beams of Gregorian antenna with θ_s=46º for feed position error of 7.5 cm (a) at focus, (b) Y_f, (c) X_f, (d) Z_f direction.

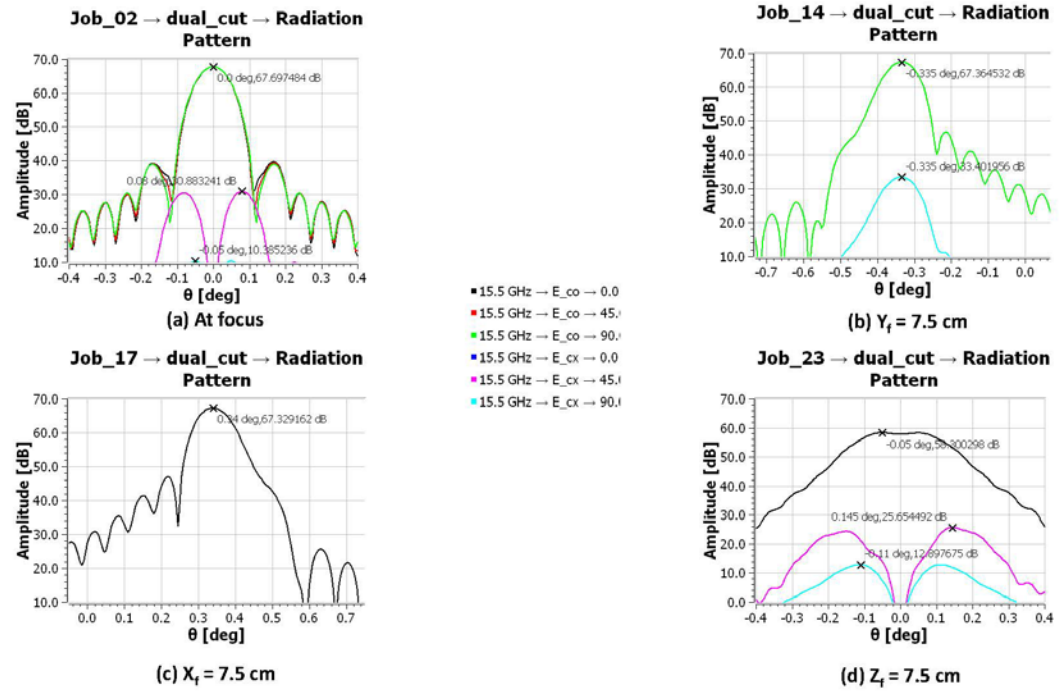

Figure 19. Beams of Gregorian antenna with θ_s=41º for feed position error of 7.5 cm (a) at focus, (b) Y_f, (c) X_f, (d) Z_f direction.

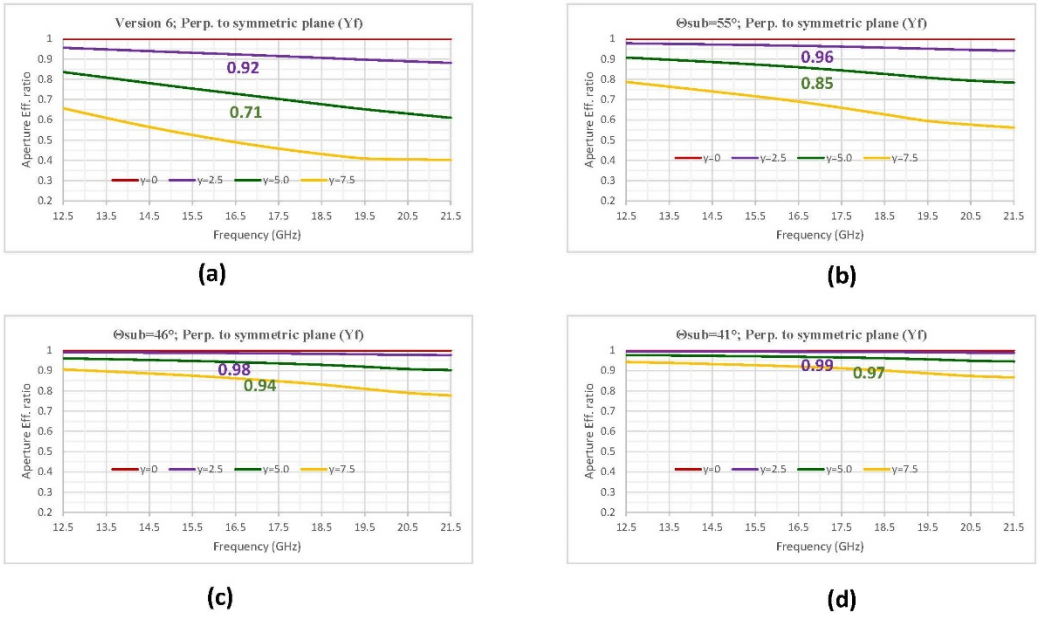

Figure 20. Normalized efficiency for offsets in asymmetric plane in Y_f direction (a) ngVLA antenna, (b) antenna with θ_s=55º, (c) antenna with θ_s=46º, (d) antenna with θ_s=41º.

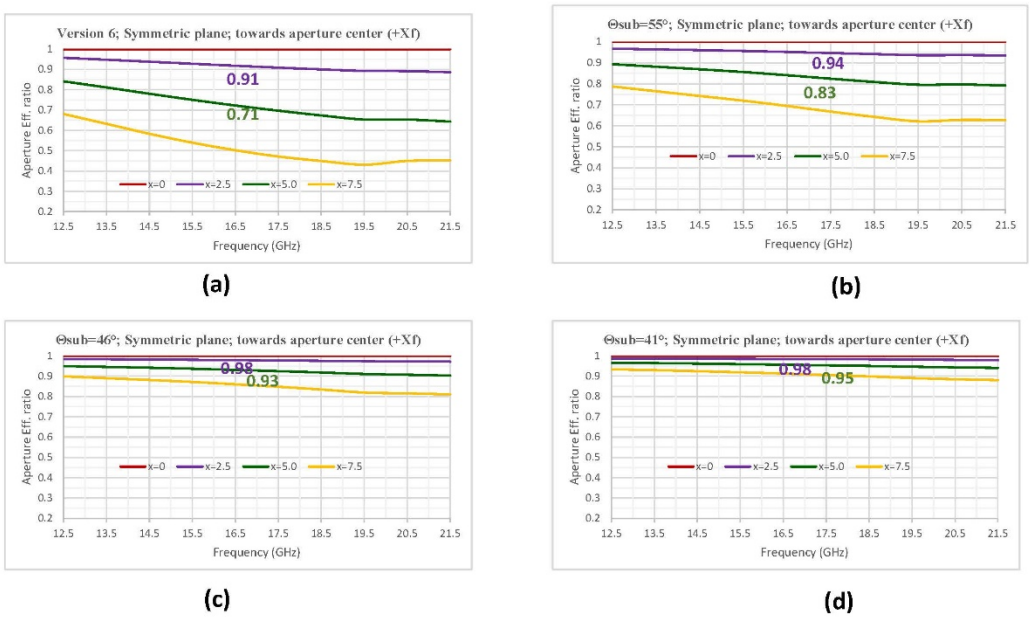

Figure 21. Normalized efficiency for offsets in symmetric plane in X_f direction (a) ngVLA antenna, (b) antenna with θ_s=55º, (c) antenna with θ_s=46º, (d) antenna with θ_s=41º.

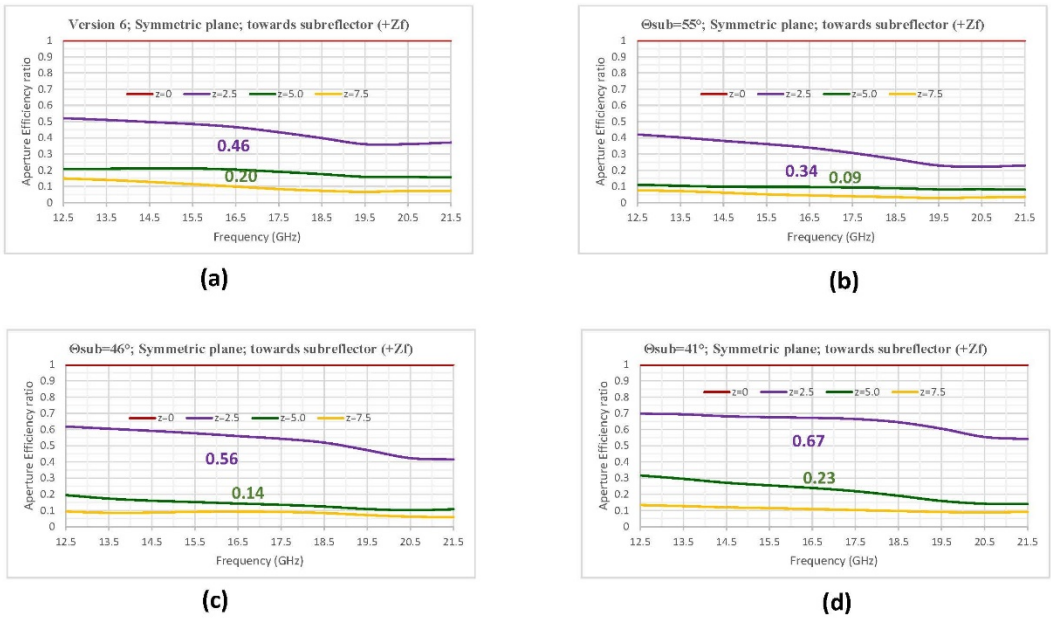

Figure 22. Normalized efficiency for offsets in symmetric plane in Z_f direction (a) ngVLA antenna, (b) antenna with θ_s=55º, (c) antenna with θ_s=46º, (d) antenna with θ_s=41º.

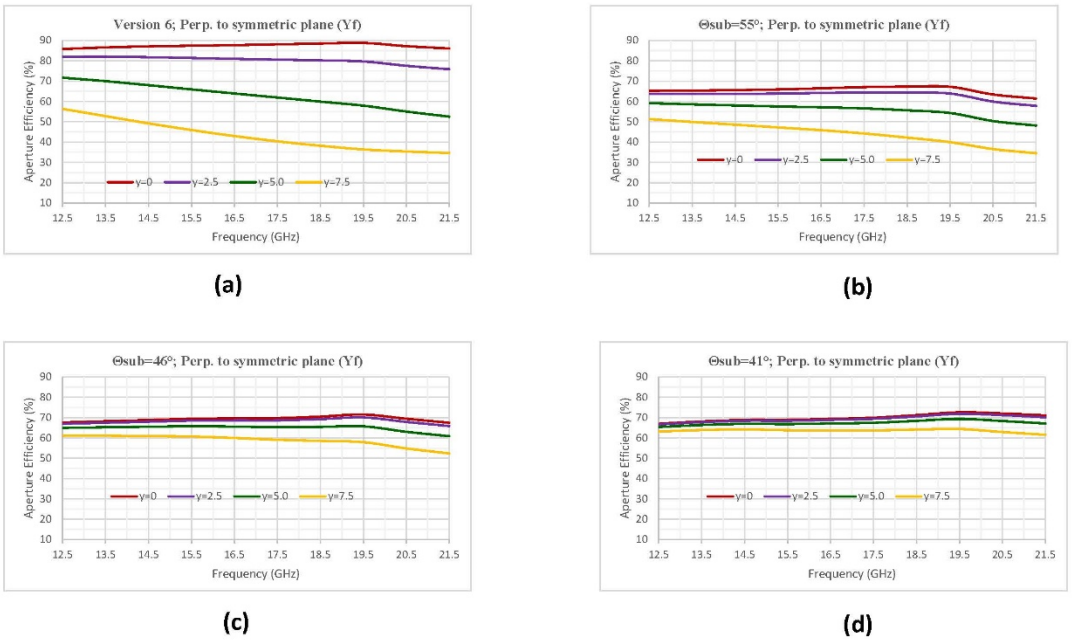

Figure 23. Efficiency for offsets in asymmetric plane in Y_f direction (a) ngVLA antenna, (b) antenna with θ_s=55º, (c) antenna with θ_s=46º, (d) antenna with θ_s=41º.

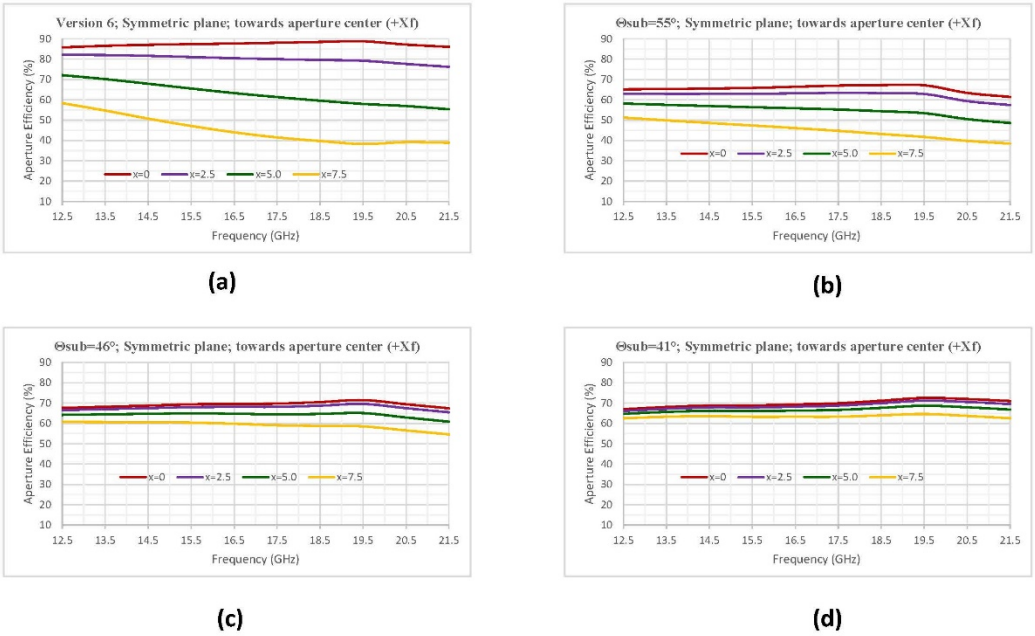

Figure 24. Efficiency for offsets in symmetric plane in X_f direction (a) ngVLA antenna, (b) antenna with θ_s=55º, (c) antenna with θ_s=46º, (d) antenna with θ_s=41º.

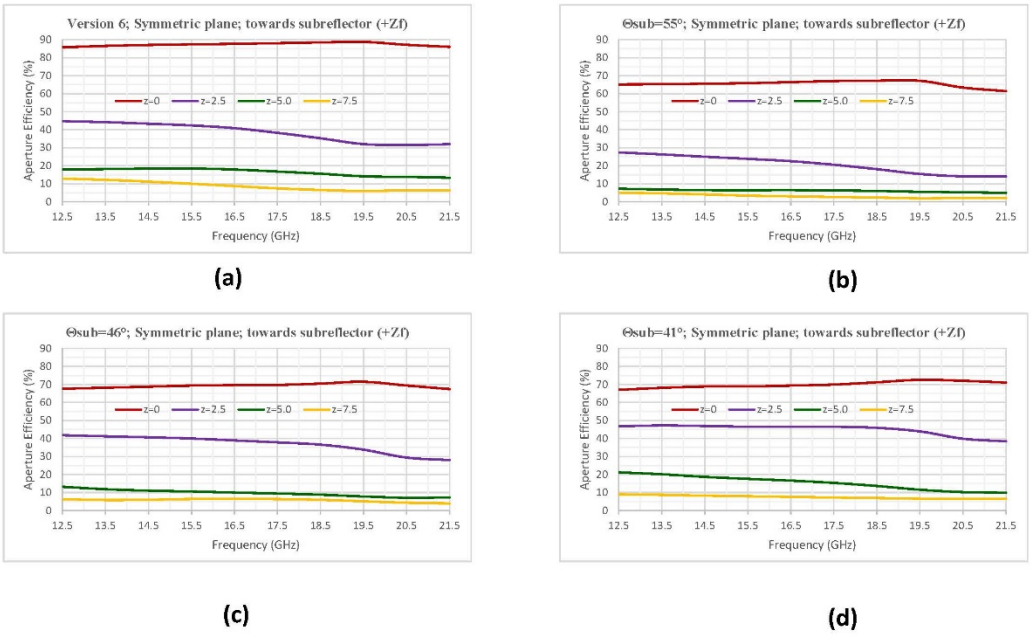

Figure 25. Efficiency for offsets in symmetric plane in Z_f direction (a) ngVLA antenna, (b) antenna with θ_s=55º, (c) antenna with θ_s=46º, (d) antenna with θ_s=41º.